STUDY OF HARD X-RAY BREMSSTRAHLUNG AT THE RADIATION-BEAM COMPLEX "TEMP"

A.B. Batrakov, E.G. Glushko, A.M. Yegorov, A.A. Zinchenko, Yu.F. Lonin, A.G. Ponomaryov, A.V. Rybka, S.I. Fedotov,V.T. Uvarov
National Science Center "Kharkov Institute of Physics and Technology", Kharkov, Ukraine
E-mail: batrakov@kipt.kharkov.ua

The basic parameters of the hard x-ray bremsstrahlung (XRB) for microsecond relativistic electron beam accelerators "TEMP" are calculated. The optimization of converters designed for this purpose has been carried out. The maximum XRB doses at the beam-radiation complex "TEMP" were experimentally obtained. The XRB radiation diagrams as a function of the beam energy and electrode configuration are taken.

PACS:41.75.Ht; PACS:41.50.+h

INTRODUCTION

Development and introduction of special gamma-ray sources and elaboration of a beam-radiation method is an important direction in the high-current accelerator technology. Advancement of these research works is evoked by a whole series of investigations into the physical-mechanical properties of structural materials, metals and alloys with the use of relativistic electron beams (REB) [1, 2]. Investigations of a radiation effect on the reactor material, simulation of reactor core conditions, study of the behavior and resistance of available materials and those being developed for the nuclear power engineering is a one more direction in investigations of hard X-ray bremsstrahlung (XRB).

Generation of XBR is carried out at two high-current relativistic electron beam accelerators "Temp-A" and "Temp-B" [3] which constitute the beam-radiation facility "TEMP" (BRF "TEMP").

The purpose of this study was: generation of XRB at BRF "TEMP"; plotting and studying of XRB radiation diagrams; investigation of XRB as a function of REB energy, vacuum diode electrode configuration, converter material and thickness.

THEORETICAL PROCEDURES

In this part the evaluation data on the X-ray bremsstrahlung parameters are r for the accelerator "Temp-B": E = (0.5…1,0) MeV, I = (10…25) kA, $\tau \approx 1.5$ μs and for the accelerator "Temp-A": E = (0.3…0.5) MeV, I = (2…3) kA, $\tau \approx 4$ μs.

Dose quantities for the continuous REB were calculated from the simplified empirical formulas [4]

$$D = 0{,}8 \cdot 10^{-3} \frac{W_e}{R^2} \cdot E^{1{,}7} \cdot \sqrt{\frac{Z_M}{13}} \ [\text{r}], \qquad (1)$$

$$\dot{D} = 0{,}8 \cdot 10^{3} \frac{\mathrm{i}_e}{R^2} \cdot E^{2{,}7} \cdot \sqrt{\frac{Z_M}{13}} \ [\text{P/s}], \qquad (2)$$

where W_e denotes the electron beam energy (J), E – the electron energy (MeV), R – the distance from the target (M), i_e – the beam current (A), Z_M – the atomic number of target.

The calculation results for the exposure dose D and its power $\dot{D}$ at different distances R from the tungsten target (Z_M=74) for different beam energies are given in Table 1.

Table 1

Accelerator "Temp-B" (0.75 MeV)							
R, mm	5	15	25	50	80	100	120
D, r	$5.6 \cdot 10^4$	$6.3 \cdot 10^3$	$2.3 \cdot 10^3$	$5.6 \cdot 10^2$	$2.2 \cdot 10^2$	$1.4 \cdot 10^2$	$9.8 \cdot 10^1$
$\dot{D}$, r/sec	$3.7 \cdot 10^{10}$	$4.2 \cdot 10^9$	$1.5 \cdot 10^9$	$3.7 \cdot 10^8$	$1.5 \cdot 10^8$	$9.4 \cdot 10^7$	$6.5 \cdot 10^7$
Accelerator "Temp-A" (0.4 MeV)							
R, mm	5		15		50		70
D, r	$4{,}8 \cdot 10^3$		$5.4 \cdot 10^2$		$4.8 \cdot 10^1$		$2.5 \cdot 10^1$
$\dot{D}$, r/sec	$3.2 \cdot 10^9$		$3.6 \cdot 10^8$		$3.2 \cdot 10^7$		$1.6 \cdot 10^7$

The interaction between the hard photon flux and the material leads to the radiation attenuation, and the absorbed radiation causes some changes in the material itself [15]. It is obvious that the interaction character depends on the radiation intensity.

The bremsstrahlung intensity for targets from Z-material, in which, under voltage to 1 MeV, the electrons are fully decelerated, is approximately equal to [6]

$$I_{XRB} = 3 \cdot 10^{-6} \cdot i \cdot Z \cdot U^{1{,}75} \ [\text{W}], \qquad (3)$$

where i is the beam current (mA), U is the accelerating voltage (kV).

The relative integral bremsstrahlung energy yield in the case of full electron deceleration in the target of Z-material is, according to [6],

$$\eta = \frac{I_{XBR}}{i \cdot U} = 3 \cdot 10^{-6} \cdot Z \cdot U^{0{,}75}. \qquad (4),$$

The target-converter thickness exerts a strong influence on the XRB intensity. The optimum target thickness is defined from the maximum value of the electron penetration into the material [7]

$$\delta = 10^{-5} \cdot E^{3/2} / \rho, \qquad (5)$$

where E is the electron energy (keV), ρ is the material density (g/cm^3).

The calculation results for the bremsstrahlung intensity I_{XRB}, relative energy yield η, electron penetration δ into the substance, for the targets of tungsten (Z = 74), tantalum (Z= 73) and molybdenum (Z = 42) at different values of the accelerating electron voltage U are given in Table 2.

The maximum relative XRB energy yield, measured experimentally, was ≈ 1.6%, as only one part of irradiation corresponding to the beam transport direction has been taken into account.

Table 2

Parameters	Converter material					
	tungsten		tantalum		molybdenum	
U, kV	400	750	400	750	400	750
I_{XRB}, W	$4.8\cdot 10^7$	$4.44\cdot 10^8$	$2.72\cdot 10^7$	$4.44\cdot 10^8$	$2.72\cdot 10^7$	$2.52\cdot 10^8$
η	0.016	0.030	0.009	0.0298	0.009	0.017
δ, μm	27	96.2	31.2	110	50.8	180

As the atomic number of material increases the depth of electron penetration into the target decreases, but, the bremsstrahlung intensity increases.

By selecting the converter it is necessary to take into account the efficiency of electron energy conversion in XRB [8, 9], mechanical and thermophysical properties of material which should provide a high resistance of material and its durability under extreme impulsive XRB load. The converter design selection comes to the selection of material which at a minimum thickness can withstand a maximum pulse number.

One of possible ways to increase the life time of the converter is to cool it. At the accelerator "Temp-A" the converters made on the heat pipe principle were tested. It is known that such a cooling system is very effective for stationary processes.

It has been experimentally established that for the high-current REB with energy E= (0.3…0.8) MeV the use of molybdenum converters is more preferable.

EXPERIMENTAL TECHNIQUE

Experimental investigations were carried out on microsecond relativistic electron beam accelerators "Temp-A" and "Temp-B".

A major part of our experiments was focused on the study of BRF "TEMP" radiation component parameters. The XRB radiation patterns were plotted for electron beams (tubular and continuous cylindrical) of different geometry. The experiment layout for production of continuous cylindrical (Fig. 1,a) and tubular (Fig. 2,b) electron beams is presented below.

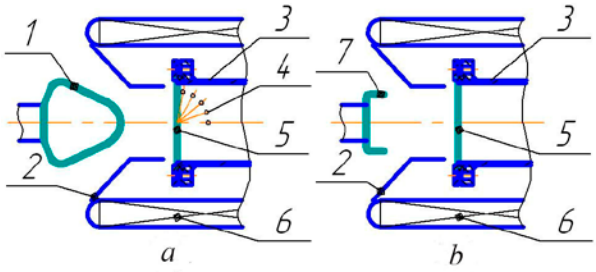

Fig. 1. Experiment layout for: a – continuous; b – tubular beam production. 1 – cone cathode; 2 – anode insertion; 3 – vacuum feed-through; 4 – X-ray probe; 5 – converter; 6 – magnetic field; 7 – edge cathode

X-ray bremsstrahlung doses have been measured with thermoluminescent sensors. Using a corresponding calibration it is possible to measure doses in a wide energy range.

Thermoluminescent LiF-based sensors of 3.5 mm diameter and 2 mm thickness were placed just behind the converter at different distances to determine the spatial X-ray radiation distribution. For targets-converters the foils from different materials (W, Mo, Ta) of a 300 μm thickness were used. The dose values each were obtained as a result of averaging a series of measurements of five shots.

A semiconductor detector was used to determine the angular distribution of the X-ray bremsstrahlung produced as a result of interaction between the continuous electron beam and the target. Typical oscillograms of investigations are shown in Fig. 2.

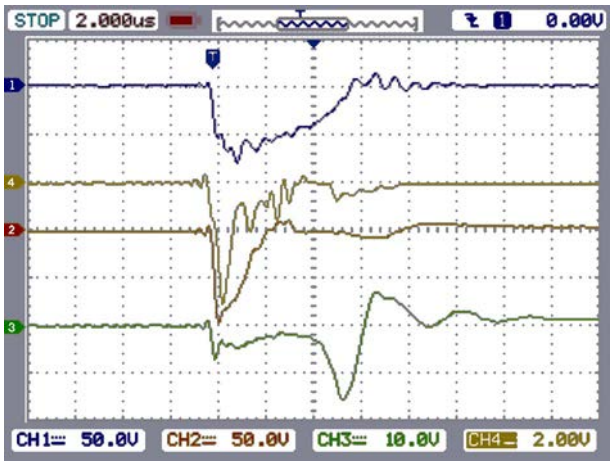

Fig. 2. Oscillograms of investigations: 1 – beam voltage; 2 – beam current; 3 – total accelerator current; 4 –X-ray probe signal

The overall dimensions of the detector are 5×5×15 mm, the resistance is $\approx 10^9$ Ohm. The signal from the semiconductor detector output is a current, created as a result of ionization in the detector, being linear relatively to the dose power independently on the temperature.

To produce a continuous relativistic electron beam the following constituents were used: cone graphite cathode with a wide part of 76 mm diameter and 68 mm length; anode insertion with an opening angle of 51 and 40 mm cone length; drift chamber of 135mm length and 70 mm diameter. The anode-cathode gap was 25 mm. The vacuum feed-through with the converter was installed behind the drift chamber. The beam indentation diameter was 25 mm. The semiconductor detectors were mounted just behind the converter at different angles to the axis (0º, 20º, 40º, 60º, 80º) on the arc of a circle of ≈ 30 mm in radius (Fig. 1,a).

Table 3 gives the measurement results for the output signals from the detectors (in volts). Measurements were carried out at the beam energy of 400 keV and 700 keV.

Table 3

Beam energy, keV	Detector position angles, º				
	0	20	40	60	80
400	3.5	2.6	2	1.7	1.3
700	12	8.4	6.1	4.8	3.4

The angular X-ray bremsstrahlung distribution diagram, obtained by the measurement results in the radiation intensity fractions in the forward direction, is shown in Fig. 3.

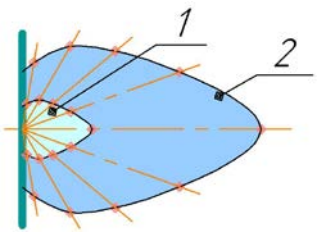

Fig. 3. XRB angular distribution diagram for a continuous beam with electron energy: 1 – 400 keV; 2 – 700 keV

The XRB angular distribution has been used for plotting the radiation diagram of XRB from the tubular REB.

Fig. 4 presents the distribution plots for calculated (Fig.4,a) and measured (Fig.4 b) doses D of REB from the continuous beam with electron energy of 0.75 MeV and 0.4 MeV.

Thermoluminescent sensors and semiconductor detectors were arranged along the beam axis at different distances R from the converter. The diagrams of Fig. 4,a,b show that the calculated and experimentally measured data are in a good agreement.

The angular distribution of XRB from the continuous cylindrical electron beam has been taken as a base for plotting the XRB radiation diagrams for tubular beams at two REB accelerators.

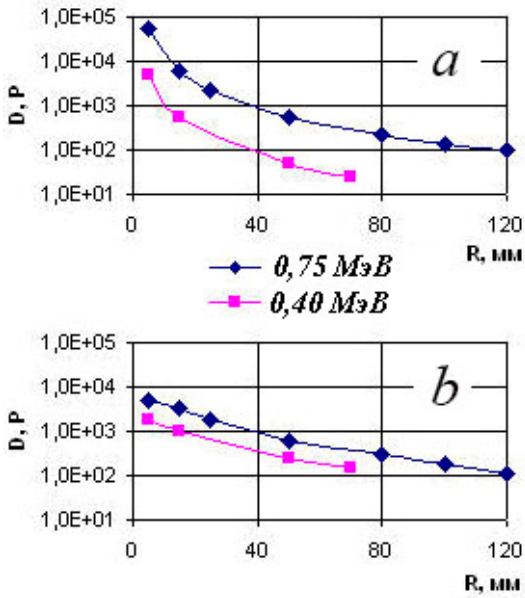

Fig. 4. Dose distribution of XRB from the continuous electron beam: a – calculated value; b – measured value

At the microsecond accelerator "Temp-A" (Fig. 5,a) the beam indentation was of ~45 mm with the beam current of (3…4) kA, electron energy of 0.35 MeV, τ ~ 5 μs, cathode diameter of 55 mm.

A tubular beam at the accelerator "Temp-B" (Fig. 5,b) was produced using the cylindrical edge cathode of 96 mm in diameter, edge height of 15 mm and edge thickness of 1 mm. The cathode-anode gap was 25 mm. The beam indentation diameter on the target was 54 mm. The beam parameters were: I = 21.5 kA, E = 750 keV, pulse duration = 1.5 μm.

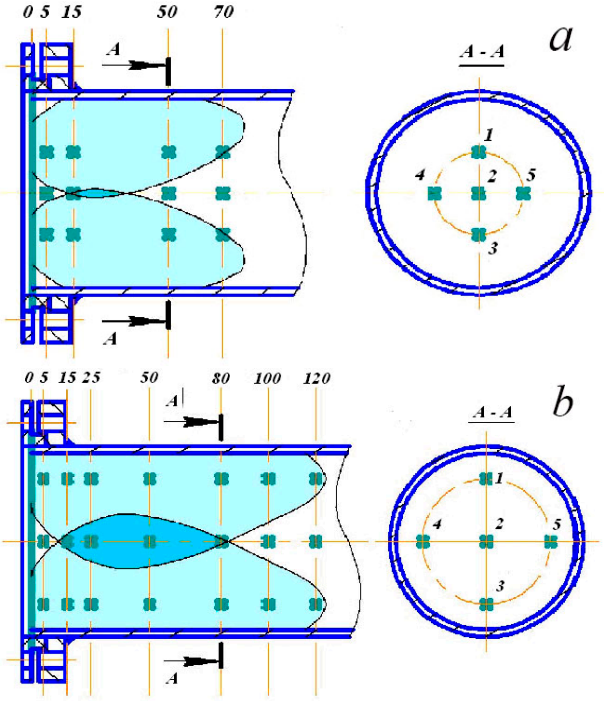

Fig. 5. XRB radiation diagrams for tubular beams with electron energy: a – E ≈ 350 keV; b – E ≈ 750 keV

The tubular beam XRB exposure doses measured at different distances from the converter and for different energies (E≈ 350 keV and E≈ 750 keV) are given in Tables 4 and 5 respectively.

Table 4

Sensors No	Distance from the converter, mm				
	5	15	25	70	
1	$6.6\cdot10^3$	$4.8\cdot10^2$	$3.3\cdot10^2$	$2.5\cdot10^2$	Dose, r
2	$2.9\cdot10^2$	$9.6\cdot10^2$	$2.1\cdot10^2$	$1.1\cdot10^2$	
3	$6.0\cdot10^3$	$4.4\cdot10^2$	$3.5\cdot10^2$	$2.6\cdot10^2$	
4	$6.3\cdot10^3$	$5.1\cdot10^2$	$2.9\cdot10^2$	$2.0\cdot10^2$	
5	$5.9\cdot10^3$	$4.0\cdot10^2$	$3.0\cdot10^2$	$2.8\cdot10^2$	

As is seen from Table 4 and 5 for LiF sensor No2, arranged along the axis of the both accelerators at a distance of 15 mm from the converter, the XRB dose increases due to the circular beam geometry.

Table 5

Sensors No	Distance from the converter, mm							
	5	15	25	50	80	100	120	
1	$9.1\cdot10^3$	$1.2\cdot10^3$	$8.4\cdot10^2$	$6.1\cdot10^2$	$3.5\cdot10^2$	$2.0\cdot10^2$	$1.2\cdot10^2$	Dose, r
2	$6.2\cdot10^2$	$1.4\cdot10^3$	$2.9\cdot10^3$	$4.1\cdot10^3$	$9.5\cdot10^2$	$6.1\cdot10^1$	$2.3\cdot10^1$	
3	$9.9\cdot10^3$	$1.4\cdot10^3$	$8.0\cdot10^2$	$5.8\cdot10^2$	$4.2\cdot10^2$	$2.7\cdot10^2$	$1.5\cdot10^2$	
4	$8.8\cdot10^3$	$1.3\cdot10^3$	$7.9\cdot10^2$	$6.3\cdot10^2$	$3.7\cdot10^2$	$1.8\cdot10^2$	$1.0\cdot10^2$	
5	$9.4\cdot10^3$	$1.0\cdot10^3$	$8.5\cdot10^2$	$6.8\cdot10^2$	$2.9\cdot10^2$	$2.9\cdot10^2$	$1.4\cdot10^2$	

ISSN 1562-6016. ВАНТ. 2015. №6(100)

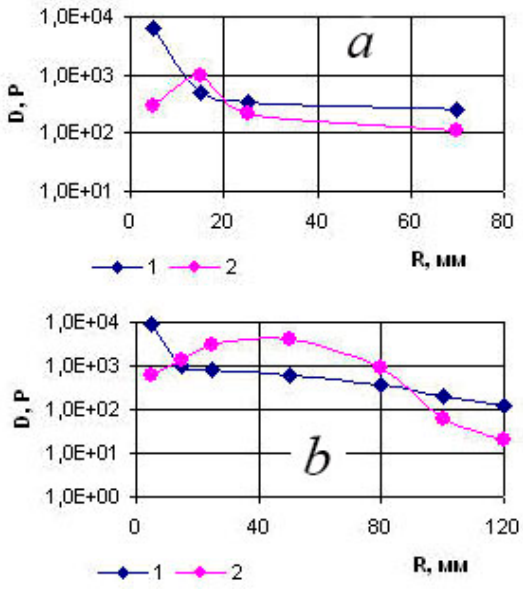

Fig.6. Tubular beam XRB dose distribution for electrons with energy: a – 0.35 MeV; b – 0.75 MeV

In the XRB dose distribution diagram (Fig. 6,a,b), plotted using the data from Tables 4 and 5, curve 1 corresponds to the XRB dose distribution by the averaged values obtained from sensors No1, No3-5 on the beam radius, and curve 2 was plotted by the XRB dose values obtained from sensor No2 arranged along the accelerator axis. The curves shows that zones and regions of the increased XRB dose for the tubular beam are strongly dependent on the electron energy.

CONCLUSIONS

1. The hard XRB doses per one REB pulse are determined for the high-current accelerators "Temp-A" and "Temp-B".

2. The XRB radiation diagrams for different electron beam geometries (continuous and tubular) are calculated and experimentally plotted using various methods.

3. The value and area occupied by XRB is strongly dependent on the accelerating voltage value.

4. It has been experimentally shown that in the accelerator near-axial region at a distance of 50 ± 20 mm from the converter the XRB dose of a tubular REB is twice much as compared to that of a continuous REB with the same intensity.

5. The results obtained give a wealth of possibilities for investigation of the XRB influence on different materials in the radiation-beam facility "TEMP".

The study is fulfilled under the NMRI X-5-527 and NANO project N 62/15 –N.

REFERENCES

1. A.V. Pashchenko, A.G. Ponomaryov, V.T Uvarov, et al. Remote coating deposition with high-current relativictic electron beams // *Khimiya i Fizika Obrabotki Materialov*. 2006, № 3, p. 24-28 (in Russian).
2. Yu.F. Lonin, V.V. Litvinenko, V.T. Uvarov, et al. The use of microsecond high-current REB for forming the hardening coatings // *Problems of Atomic Science and Technology, Series "Nuclear Physics Experiments"*. 2008, № 5, p. 91-95.
3. Yu.F. Lonin, I.I. Magda. High-current relativistic accelerators at IPENAM NSC KIPT and their application // *Problems of Atomic Science and Technology, Series "Nuclear Physics Experiments" (50),* 2008, № 5, p. 85-90.
4. V.M. Fedotov. *Measuring the electron energy of high-current megavolt beams by the hardness of x-ray radiation from the thick target:* Preprint 86-40. Novosibirsk: Institute of Nuclear Physics SO AS of USSR, 1968, p. 14.
5. V.N. Bojko, A.N. Valyayev, A.D. Pogrebnyak. Metal material modification with pulsed powerful particle beam // *Uspekhi Fizicheskikh Nauk*. 1999, v. 169, p. 1243-271 (in Russian).
6. R. Yeger. *Dosimetry and radiation protection.* M.: «Gosatomizdat», 1961 (in Russian).
7. V.F. Kovalenko. On calculation of electron penetration depth // *Ehlectronnaya Tekhnika. Seriya 1. Microwave Ehlektronika*. 1972, № 1, p. 3-11 (in Russian).
8. Yu.F. Lonin, A.G. Ponomaryov, G.E. Sarukhanyan, A.B. Batrakov, V.T. Uvarov, L.N. Kazban, V.T. Lazurik. Investigation of the bremsstrahlung yield at the high-current relativistic electron beam accelerators in IPENAM // *Problems of Atomic Science and Technology, Series "Plasma Electronics and New Acceleration Methods"*. 2012, № 4, p. 163-166.
9. A.B. Batrakov, S.P. Bondarenko, Yu.F. Lonin, A.G. Ponomaryov, G.V. Sotnikov. Optimization of relativistic electron beam parameters for high-power X-ray bremsstrahlung generation // *Problems of Atomic Science and Technology, Series "Plasma Electronics and New Acceleration Methods"*. 2010, №4, p. 21-24.
10. A.V. Rybka, I.M. Prokhorets, I.N. Shlyakhov, A.A. Zakharchenko, A.A. Blinkin, L.N. Davydov, M.A. Kuzmichov, D.V. Kutnij, A.N. Orobinsky, N.I. Kravchenko. Dosimetric characteristics of CdZnTe-based X-ray and gamma-ray detectors // *Problems of Atomic Science and Technology. Series "Radiation damage physics and radiation material science"*. 2000, № 4(78), p. 208-211.

Article received 26.10.2015

ИССЛЕДОВАНИЕ ЖЕСТКОГО ТОРМОЗНОГО РЕНТГЕНОВСКОГО ИЗЛУЧЕНИЯ НА РАДИАЦИОННО-ПУЧКОВОМ КОМПЛЕКСЕ «ТЕМП»

А.Б. Батраков, Е.Г. Глушко, А.М. Егоров, А.А. Зинченко, Ю.Ф. Лонин, А.Г. Пономарев, А.В. Рыбка, С.И. Федотов, В.Т. Уваров

Приведен расчет основных параметров жесткого тормозного рентгеновского излучения (ТРИ) для микросекундных ускорителей релятивистских электронных пучков (РЭП) «ТЕМП». Проведена оптимизация конверторов для этих целей. Экспериментально получены максимальные дозы ТРИ на пучково-радиационном комплексе «ТЕМП». Сняты диаграммы направленности ТРИ в зависимости от энергий пучков и форм электродов.

ДОСЛІДЖЕННЯ ЖОРСТКОГО ГАЛЬМІВНОГО РЕНТГЕНІВСЬКОГО ВИПРОМІНЮВАННЯ НА РАДІАЦІЙНО-ПУЧКОВОМУ КОМПЛЕКСІ «ТЕМП»

О.Б. Батраков, Е.Г. Глушко, О.М. Єгоров,А.О. Зінченко, Ю.Ф. Лонін, А.Г. Пономарьов, А.В. Рибка, С.І. Федотов, В.Т. Уваров

Наведено розрахунок основних параметрів жорсткого гальмівного рентгенівського випромінювання (ГРВ) для мікросекундних прискорювачів релятивістських електронних пучків «ТЕМП». Проведено оптимізацію конверторів для цього. Експериментально отримано максимальні дози ГРВ на радіаційно-пучковому комплексі «ТЕМП». Знято діаграми напрямку ГРВ в залежності від енергії пучків та форми електродів.